NJC

Accepted Manuscript

This is an *Accepted Manuscript*, which has been through the Royal Society of Chemistry peer review process and has been accepted for publication.

Accepted Manuscripts are published online shortly after acceptance, before technical editing, formatting and proof reading. Using this free service, authors can make their results available to the community, in citable form, before we publish the edited article. We will replace this *Accepted Manuscript* with the edited and formatted *Advance Article* as soon as it is available.

You can find more information about *Accepted Manuscripts* in the Information for Authors.

Please note that technical editing may introduce minor changes to the text and/or graphics, which may alter content. The journal's standard Terms & Conditions and the Ethical guidelines still apply. In no event shall the Royal Society of Chemistry be held responsible for any errors or omissions in this *Accepted Manuscript* or any consequences arising from the use of any information it contains.

ROYAL SOCIETY OF CHEMISTRY

www.rsc.org/njc

A boron dipyrromethene-based fluorescent probe for sensing HOCl was developed .

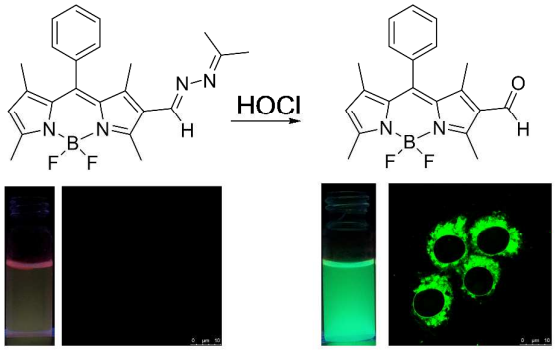

A turn-on fluorescent probe for hypochlorous acid based on HOCl-promoted removal of the C=N bond in BODIPY-hydrazone

Wei-Chieh Chen[a], Parthiban Venkatesan[a], Shu-Pao Wu[a,]*

[a] Department of Applied Chemistry, National Chiao Tung University, Hsinchu, Taiwan 300, ROC. E-mail: spwu@mail.nctu.edu.tw. Tel.: +886-3-5712121-ext56506; Fax: +886-3-5723764

*Corresponding author.

Abstract

A boron dipyrromethene-based fluorescent probe, **BODH**, has been successfully developed for hypochlorous acid detection based on HOCl-promoted oxidative removal of the C=N bond in response to the amount of HOCl. The reaction is accompanied by a 6-fold increase in the fluorescent quantum yield (from 0.05 to 0.29). The fluorescence intensity of the reaction between HOCl and **BODH** shows a good linearity in the HOCl concentration range of 1 to 25 μM with a low detection limit of 205 nM (S/N = 3). Confocal fluorescence microscopy imaging using RAW264.7 cells shows that the new probe **BODH** can be used as an effective fluorescent probe for detecting HOCl in living cells.

Keywords: Hypochlorous acid; Fluorescent probe; Boron dipyrromethene; Bioimaging.

1. Introduction

Hypochlorous acid (HOCl) is a reactive oxygen species (ROS) produced as a defense mechanism in the immune system.[1-4] Endogenous hypochlorous acid is formed from the reaction of chloride ion with hydrogen peroxide catalyzed by the enzyme myeloperoxidase (MPO) in leukocytes including macrophages, monocytes, and neutrophils.[5,6] However, overproduction of HOCl causes several human diseases such as arthritis, cancer and neurodegeneration.[7-9] Due to its biological importance, the need to design highly sensitive and selective probes for HOCl has become a significant research issue. Fluorescent probes that can directly indicate the change in concentration of HOCl would be useful for examining the dynamic spreading of HOCl in living cells.

HOCl has shown high oxidation properties, which can be used to design a probe for HOCl. Several functional groups, such as p-methoxyphenol, oxime, selenide, telluride and thiol, have been found to be HOCl-reactive moieties.[10-33] To construct a HOCl fluorescent probe, a HOCl-reactive moiety is connected to an organic fluorophore so that it can control the fluorescence of the fluorophore. In particular, the isomerization of the C=N group is known to undergo non-radiative decay in the excited state; this can be used as a signal alteration for fluorescence turn-on sensing.[11] In the absence of HOCl, the fluorescence of the fluorophore is quenched due to imine

isomerization; however, in the presence of HOCl, the imine isomerization is blocked by HOCl oxidation and the fluorescence of the fluorophore is reestablished. To facilitate the practical application of HOCl probes in cell imaging, development of these probes has focused on selectivity and sensitivity. In this paper, we have reported a highly sensitive and selective fluorescent probe for HOCl based on the HOCl-promoted oxidation of imine.

In this work, a BODIPY-based fluorescent probe **BODH**, was designed for HOCl detection based on HOCl-promoted removal of the C=N bond. **BODH** displays weak fluorescence with a quantum yield of Φ = 0.05 due to imine (C=N) isomerization, which has been known to exhibit non-radiactive decay in the excited state. The strong fluorescence of BODIPY is restored after the imine bond is oxidized to aldehyde (R-CHO) by HOCl. This new probe exhibits high selectivity and sensitivity towards HOCl over other ROS and reactive nitrogen species (RNS) in aqueous solutions. Most importantly, **BODH** shows good cell-membrane permeability and can be successfully used to obtain images of endogenous HOCl in living cells.

2. Experimental

2.1Materials and Instrumentation

All reagents were obtained from commercial sources and used as received without further purification. UV/Vis spectra were recorded on an Agilent 8453 UV/Vis

spectrometer. Fluorescence spectra measurements were performed on a Hitachi F-7000 fluorescence spectrophotometer. NMR spectra were obtained on a Bruker DRX-300 and Agilent Unity INOVA-500 NMR spectrometer. Fluorescent images were taken on a Leica TCS SP5 X AOBS Confocal Fluorescence Microscope.

2.2 Preparation of ROS and RNS

Various ROS and RNS including HOCl, $^{\bullet}OH$, H_2O_2, $^1O_2$, NO_2^-, NO_3^-, NO, $ONOO^-$, O_2^- and *t*-BuOOH were prepared according to the following methods. HOCl was prepared from NaOCl; the concentration of hypochlorite (OCl^-) was determined by using an extinction coefficient of 350 $M^{-1}cm^{-1}$ (292 nm) at pH 9.0. Hydroxyl radical ($^{\bullet}OH$) was generated by Fenton reaction on mixing $Fe(NH_4)_2(SO_4)_2 \cdot 6H_2O$ with 10 equivalents of H_2O_2; the concentration of $^{\bullet}OH$ was estimated from the concentration of Fe^{2+}. The concentration of the commercially available stock H_2O_2 solution was estimated by optical absorbance at 240 nm. Singlet oxygen ($^1O_2$) was generated by the addition of NaOCl and H_2O_2 according to the literature.[34] The source of NO_2^- and NO_3^- was from $NaNO_2$ and $NaNO_3$. Nitric oxide (NO) was generated from sodium nitroferricyanide(III) dihydrate. Peroxynitrite ($ONOO^-$) was prepared as the reported method;[35] the concentration of peroxynitrite was estimated by using an extinction coefficient of 1670 $M^{-1}cm^{-1}$ (302 nm). Superoxide (O_2^-) is prepared from KO_2. *t*-BuOOH was obtained commercially from Alfa Aesar.

2.3 Synthesis of BODH

Hydrazine (99%, 172.12 μL, 2.8 mmol) in MeOH was added to a solution of BODIPY-aldehyde (100 mg, 0.28 mmol) in THF/MeOH (5 mL / 30 mL). The reaction mixture was stirred for 12 h at room temperature. The solvent was removed under reduced pressure and the solid was dissolved in acetone (30 mL) and then further stirred for 12 h. The solvent was removed under reduced pressure and the solid was taken up into a mixture of water and CH_2Cl_2. The mixture was extracted four times with EtOAc. The combined organic fractions were dried over $MgSO_4$, and then the solvent was removed under reduced pressure. The crude material was purified by column chromatography (hexane: CH_2Cl_2 = 1:1) to give the compound as a dark purple solid. Yield: 60.5 mg (53 %). m.p. 187.3 °C. ^{1}H NMR (300 MHz, $CDCl_3$): δ 8.43 (s, 1H), 7.53-7.51 (m, 3H), 7.32-7.28 (m, 2H), 6.08 (s, 1H), 2.85 (s, 3H), 2.61 (s, 3H), 2.11 (s, 6H), 1.59 (s, 3H), 1.40 (s, 3H). ^{13}C NMR (125 MHz, $CDCl_3$): δ 167.8, 158.1, 155.8, 152.7, 145.0, 142.4, 141.5, 134.7, 132.5, 130.6, 129.2, 129.1, 127.9, 123.9, 122.5, 29.6, 25.2, 18.6, 14.6, 14.4, 14.2, 12.2. HRMS (EI^+): calcd. for $C_{23}H_{25}BF_2N_4$ $[M]^+$ 406.1240; found 406.1247.

2.4 Cell Culture for RAW264.7 Macrophages

The cell line RAW264.7 was provided by the Food Industry Research and Development Institute (Taiwan). RAW264.7 cells were cultured in Dulbecco's modied Eagle's medium (DMEM) supplemented with 10% fetal bovine serum (FBS) at 37 °C under an atmosphere of 5% CO_2. Cells were plated on 18 mm glass coverslips and allowed to adhere for 24 h.

2.5 Cytotoxicity assay

The methyl thiazolyl tetrazolium (MTT) assay was used to measure the cytotoxicity of **BODH** in RAW264.7 cells. RAW264.7 cells were seeded into a 96-well cell-culture plate. Various concentrations (5, 10, 15, 20, 25 μM) of **BODH** were added to the wells. The cells were incubated at 37℃ under 5% CO_2 for 24 h. 10 μL MTT (5 mg/mL) was added to each well and incubated at 37°C under 5% CO_2 for 4 h. Remove the MTT solution and yellow precipitates (formazan) observed in plates were dissolved in 200 μL DMSO and 25 μL Sorenson's glycine buffer (0.1 M glycine and 0.1 M NaCl). Multiskan GO microplate reader was used to measure the absorbance at 570 nm for each well. The viability of cells was calculated according to the following equation:

Cell viability (%) = (mean of absorbance value of treatment group) / (mean of absorbance value of control group).

2.6 Fluorescence Imaging of Exogenous BODH in Living Cells

Experiments to assess the sensing ability of **BODH** for exogenous NaOCl were performed in 0.1 M phosphate-buffered saline (PBS) with NaOCl (10 μM). Treat the cells with 2 μL of 10 mM **BODH** (final concentration: 10 μM) dissolved in DMSO and incubated for 30 min at 37 °C. The treated cells were washed with 0.1 M PBS (2 mL × 3) to remove remaining **BODH**. DMEM (2 mL) was added to the cell culture, which was then treated with 10 mM solution of NaOCl (2 μL; final concentration: 10 μM) dissolved in sterilized 0.1 M PBS (pH 7.4). The samples were incubated at 37 ˚C for 10 min. The culture medium was removed, and the treated cells were washed with 0.1 M PBS (2 mL × 3). Paraformaldehyde solution (1 mL, 4%, in PBS) was added to the treated cell and keep in room temperature 20 min for cell fixation. The Paraformaldehyde solution was removed and the treated cells were washed with 0.1 M PBS (2 mL × 3) and DI water (2 mL× 3). The cell specimen was made before observation. Confocal fluorescence imaging of cells was performed with a Leica TCS SP5 X AOBS Confocal Fluorescence Microscope (Germany), and a 63x oil-immersion objective lens was used. The cells were excited with a white light laser at 470 nm, and emission was collected at 495-535 nm.

2.7 Fluorescence Imaging of PMA-Induced BODH Production in Living Cells

RAW264.7 cells were treated with PMA (25 ng/mL) and **BODH** in culture medium for 2 h. The culture medium was removed, and the treated cells were washed with 0.1 M PBS (2 mL × 3) before observation. Fluorescence imaging was performed with a Leica TCS SP5 X AOBS Confocal Fluorescence Microscope. The cells were excited with a white light laser at 480 nm, and emission was collected at 495-535 nm.

3. Results and discussion

3.1 Synthesis of the probe BODH

The synthesis of the probe **BODH** is outlined in Scheme 1. BODIPY-aldehyde was obtained from the formylation reaction of BODIPY with Vilsmeier-Haack reagent (DMF / $POCl_3$). In the next step, the BODIPY-aldehyde was further treated with hydrazine, followed by acetone. The structure of **BODH** was confirmed using ^{1}H NMR, ^{13}C NMR and high resolution EI MS. The probe **BODH** was pink and had an absorption band centered at 535 nm, which was red-shifted by 50 nm from the typical BODIPY absorption band at 480 nm, due to longer conjugated double bonds. The probe **BODH** exhibited weak fluorescence ($\Phi = 0.05$) compared to BODIPY ($\Phi = 0.6–0.9$) due to imine (C=N) isomerization, which exhibits non-radiactive decay in the excited state.

3.2 Fluorescent response of BODH with HOCl

The sensing ability of the probe **BODH** was tested for various ROS and RNS, including NaOCl, $^{\bullet}OH$, H_2O_2, $^1O_2$, NO_2^-, NO_3^-, NO, $ONOO^-$, O_2^-, and *t*-BuOOH, in a phosphate-buffered saline (PBS) solution. It was found that strong green fluorescence emission only occurred for the addition of HOCl to the **BODH** solution; other ROS and RNS produced no change in fluorescence (Fig. 1). Quantitative fluorescence spectra of **BODH** were recorded in the presence of several ROS and RNS, but HOCl was the only reactive species to cause an obvious fluorescence enhancement (Fig. 2). The reaction of **BODH** with HOCl was fast; addition of NaOCl(aq) to the solution of the probe **BODH** within 3 min caused a significant change in fluorescence intensity (see Figure S5 in the supporting information). During NaOCl titration with **BODH**, the absorbance at 512 nm decreased and a new band at 492 nm appeared (Fig. 3). The oxidized product, **BODIPY-Al**, has a shorter absorption wavelength centered at 492 nm, which is blue-shifted by 20 nm from the absorption band of **BODH** at 512 nm (Scheme 2). This is due to shorter double bond conjugation in the oxidized product, **BODIPY-Al**. This absorption change was also observed as color change from pink to red (Fig. 1). In addition, upon gradual addition of HOCl to a solution of **BODH,** an emission band centered at 508 nm was formed (Fig. 3). The emission intensity reached its maximum after the addition of four equivalents of NaOCl.

BODH displays weak fluorescence with a quantum yield of Φ = 0.05 due to imine (C=N) isomerization, which has been known to exhibit non-radiactive decay in the excited state. The strong fluorescence of BODIPY is restored after the oxidation of imine to aldehyde (R-CHO) by HOCl (Scheme 2). The quantum yield of the oxidized **BODH** was Φ = 0.29, which is 6-fold higher than that of **BODH**, at Φ = 0.05. The structure of oxidized **BODH** was confirmed by ^{1}H NMR, ^{13}C NMR, HPLC, and MS spectrometry. ^{1}H NMR spectra of **BODH** showed that the proton (H_a, imine) signal at δ = 8.41 ppm disappeared as NaOCl was added and a new peak at δ = 10.03 ppm was formed (Fig. 4). This indicates that the oxidization of **BODH** by NaOCl happens on the imine group. According to the MS and NMR spectra of oxidized **BODH**, the imine group was oxidized to be an aldehyde group (CHO). Notably, there was a good linear correlation between the fluorescence intensity and the concentration of NaOCl (0 – 20 μM). Furthermore, it was found that **BODH** had a detection limit of 0.205 μM (see Figure S7 in the supporting information), which makes it sufficiently sensitive for HOCl detection in living systems.

A pH-dependence experiment was conducted with **BODH**, to investigate a suitable pH range for HOCl sensing. Fig. 5 shows that the emission intensities of **BODH** are very low at a pH range of 4.5 – 10. After addition of NaOCl, the emission intensity at 508 nm became significantly higher at a pH range of 5.0 – 10.0, which means that the

probe could be used in physiological conditions. The emission enhancement is much more pronounced under basic conditions (pH > 7) than under acidic conditions (pH < 7), implying that hypochlorite (ClO^-) plays a key role in the sensing process.

3.3 Imaging live cells

The potential of the probe **BODH** for imaging HOCl in living cells was investigated. Murine RAW264.7 macrophages were used as a model because macrophages are known to generate ROS and RNS in the immune system. First, an MTT assay with a RAW264.7 cell line was used to determine the cytotoxicity of **HBP**. In Fig. 6, the cellular viability was estimated to be greater than 80% after 24 h, which indicates that **BODH** (<30 μM) has low cytotoxicity. Furthermore, the images of cells were obtained using a confocal fluorescence microscope. When RAW264.7 cells were incubated with **BODH** (10 μM), no fluorescence was observed (Fig. 7a). After the treatment of NaOCl, bright green fluorescence was observed in the RAW264.7 cells (Figure 7b). An overlay of fluorescence and bright-field images shows that the fluorescence signals are localized in the intracellular area, indicating a subcellular distribution of HOCl and good cell-membrane permeability of **BODH**.

Finally, **BODH** was used to detect PMA-induced endogenous HOCl production in RAW264.7 cells. Phorbol myristate acetate (PMA) is known to activate the generation of ROS and RNS in macrophage cells, including HOCl.[36] After stimulation

with PMA (25 ng/mL) for 2 h in the presence of **BODH**, strong green fluorescence was observed in RAW264.7 cells (Fig. 8). These results demonstrated that **BODH** is able to visualize PMA-induced endogenous HOCl production in the macrophages. When MPO inhibitor (4-aminibenzohydrazide) was added along with PMA to RAW 264.7 cells, fluorescence enhancement was not observed. This clearly indicates that HOCl only caused fluorescence enhancement while remaining reactive oxygen species caused negligible fluorescence enhancement. In order to localize where the probe **BODH** can be used to detect endogenous HOCl production, HiLyte Fluor^{TM} 594 acid (cytosol stain) and DAPI (nuclear stain) were used. Fig. 8 shows that the staining by the probe **BODH** is identical to that by HiLyte Fluor^{TM} 594 acid. In the nuclear region, there is no **BODH** staining. These observations indicate that the probe **BODH** can be used to detect endogenous HOCl production in the cytosol.

4. Conclusion

In summary, we have developed a BODIPY-based green fluorescent probe **BODH** that exhibits a highly selective and sensitive response to HOCl over other reactive species. This system utilizes the HOCl-promoted oxidation and removal of the C=N bond to respond to the amount of HOCl. **BODH** is rapidly oxidized by HOCl to be BODIPY-Al with an emission enhancement. Confocal fluorescence

microscopy imaging using RAW264.7 cells showed that the probe **BODH** could be used to evaluate the important role of HOCl in biological systems.

Acknowledgements

We gratefully acknowledge the financial support of Ministry of Science and Technology (Taiwan, MOST 103-2113-M-009-005) and National Chiao Tung University.

Appendix A. Supplementary data

^{1}H NMR, ^{13}C NMR and mass spectra of **BODH**, the reaction profile of **BODH** with NaOCl, calibration curve of the reaction **BODH** with NaOCl.

References

1 C. C. Winterbourn, M. B. Hampton, J. H. Livesey and A. J. Kettle, *J. Biol. Chem*., 2006, **281**, 39860-39869.
2 X. Chen, X. Tian, I. Shin and J. Yoon, *Chem. Soc. Rev.*, 2011, **40**, 4783-4804.
3 S. P. Shin, M. S. Kim, S. H. Cho, J. H. Kim, C. H. Choresca Jr., J. E. Han, J. W. Jun, S. C. Park, *J. Prev. Vet. Med.*, 2013, **37**, 49-52.
4 J. Marcinkiewicz, B. Chain, B. Nowak, A. Grabowska, K. Bryniarski, J. Baran, *Inflamm. Res.*, 2000, **49**, 280–289.
5 T. J. Fiedler, C. A. Davey and R. E. Fenna, *J. Biol. Chem.*, 2000, **275**, 11964-11971.
6 Y. W. Yap, M. Whiteman and N. S. Cheung, *Cell. Signal.,* 2007, **19**, 219-228.
7 L. J. Hazell, L. Arnold, D. Flowers, G. Waeg, E. Malle and R. Stocker, *J. Clin. Invest.*, 1996, **97**, 1535-1544.
8 V. Rudolph, R. P. Andrie, T. K. Rudolph, K. Friedrichs, A. Klinke, B. Hirsch-Hoffmann, A. P. Schwoerer, D. Lau, X. Fu, K.Klingel, K. Sydow, M. Didie, A. Seniuk, E.-C. von Leitner, K. Szoecs, J. W. Schrickel, H. Treede, U. Wenzel, T. Lewalter, G. Nickenig, W.-H. Zimmermann, T. Meinertz, R. H. Boger, H. Reichenspurner, B. A. Freeman, T. Eschenhagen, H. Ehmke, S. L. Hazen, S. Willems and S. Baldus, *Nat. Med.*, 2010, **16**, 470-474.

9 M. Whiteman, P. Rose, J. L. Siau, N. S. Cheung, G. S. Tan, B. Halliwell and J. S. Armstrong, *Free Radic. Biol. Med.*, 2005, **38**, 1571-1584.
10 Z.-N. Sun, F.-Q. Liu, Y. Chen, P. K. H. Tam and D. Yang, *Org. Lett.*, 2008, **10**, 2171-2174.
11 X. Cheng, H. Jia, T. Long, J. Feng, J. Qin and Z. Li, *Chem. Commun.*, 2011, **47**, 11978-11980.
12 Y. Zhou, J.-Y. Li, K.-H. Chu, K. Liu, C. Yao and J.-Y. Li, *Chem. Commun.*, 2012, **48**, 4677-.467
13 B. Wang, P. Li, F. Yu, P. Song, X. Sun, S. Yang, Z. Lou and K. Han, *Chem. Commun.*, 2013, **49**, 1014-1016.
14 S.-R. Liu and S.-P. Wu, *Org. Lett.*, 2013, **15**, 878-881.
15 S.-R. Liu, M. Vedamalai and S.-P. Wu, *Anal. Chim. Acta.*, 2013, **800**, 71-76.
16 Q. Xu, K.-A. Lee, S. Lee, K. M. Lee, W.-J. Lee and J. Yoon, *J. Am. Chem. Soc.*, 2013, **135**, 9944-9949.
17 M. Emrullahoglu, M. Ucuncu and E. Karakus, *Chem. Commun.*, 2013, **49**, 7836-7838.
18 G. Cheng, J. Fan, W. Sun, J. Cao, C. Hu and X. Peng, *Chem. Commun.*, 2014, **50**, 1018-1020.
19 J. J. Hu, N.-K. Wong, Q. Gu, X. Bai, S. Ye and D. Yang, *Org. Lett.*, 2014, **16**, 3544-3547.
20 S. Yu, C. Hsu, W. Chen, L. Wei, S. Wu, *Sens. Actuators B*, 2014, **196**, 203-207.
21 J. Li, F. Huo and C. Yin, *RSC Advances*, 2014, **4**, 44610–44613.
22 F. Liu, Y. Gao, J. Wang and S. Sun, *Analyst*, 2014, **139**, 3324–3329.
23 J. Kim and Y. Kim, *Analyst*, 2014, **139**, 2986–2989.
24 Y. Zhang, X. Chen, J. Shao, J. Zhang, Q. Yuan, J. Miao, B. Zhao, *Chem. Commun.*, 2014, **50**, 14241-14244.
25 S. I. Reja, V. Bhalla, A. Sharma, G. Kaur, M. Kumar, *Chem. Commun.*, 2014, **50**, 11911-11914
26 J. Hou, M. Wu, K. Li, J. Yang, K. Yu, Y. Xie, X. Yu, *Chem. Commun.*, 2014, **50**, 8640-8643
27 S. Goswami, A. K. Das, A. Manna, A. K. Maity, P. Saha, C. K. Quah, H. Fun, H. A. Abdel-Aziz, *Anal. Chem.*, 2014, **86**, 6315-6322
28 H. Zhu, J. Fan, J. Wang, H. Mu, X. Peng, *J. Am. Chem. Soc.*, 2014, **136**, 12820-12823
29 J. Zhao, H. Li, K. Yang, S. Sun, A. Lu and Y. Xu, *New J. Chem.*, 2014, **38**, 3371-3374.

30 B. Zhu, Y. Xu, W. Liu, C. Shao, H. Wu, H. Jiang, B. Du, X. Zhang, *Sens. Actuat. B Chem.* 2014, **191**, 473–478.

31 Y. Yang, C. Yin, F. Huo, J. Chao, Y. Zhang, S. Jin, *Sens. Actuat. B Chem*. 2014, **199**, 226–231.

32 Z. Yang, M. Wang, M. She, B. Yin, Y. Huang, P. Liu, J. Li, S. Zhang, *Sens. Actuat. B Chem*. 2014, **202**, 656–662

33 P. Venkatesan, S. Wu, *Analyst*, 2015, **140**, 1349-1355.

34 X. Li, G. Zhang, H. Ma, D. Zhang, J. Li and D. Zhu, *J. Am. Chem. Soc.*, 2004, **126**, 11543-11548.

35 J. W. Reed, H. H. Ho and W. L. Jolly, *J. Am. Chem. Soc.*, 1974, **96**, 1248-1249.

36 Y.-C. Yang, H.-H. Lu, W.-T. Wang and I. Liau, *Anal. Chem.*, 2011, **83**, 8267-8272.

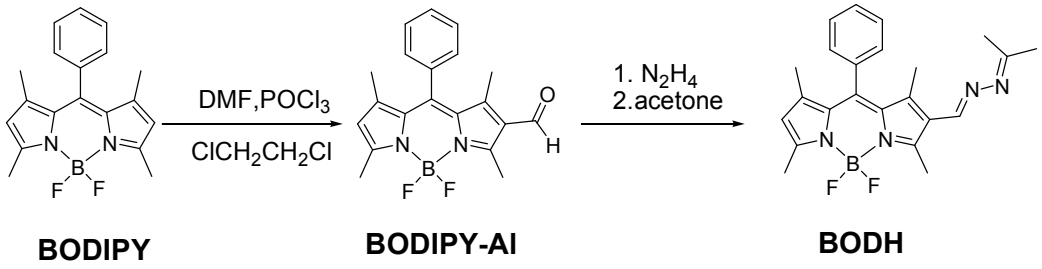

Scheme 1. Synthesis of the probe **BODH**

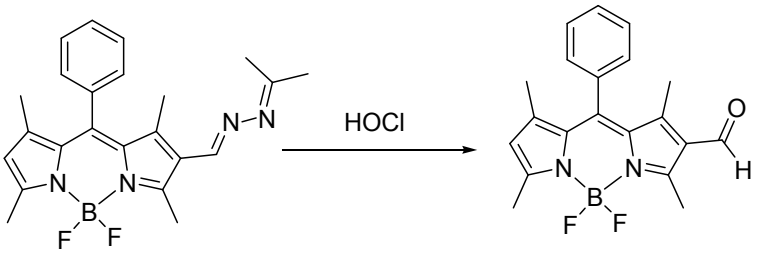

BODH **BODIPY-Al**

Scheme 2. The reaction of the probe **BODH** with HOCl

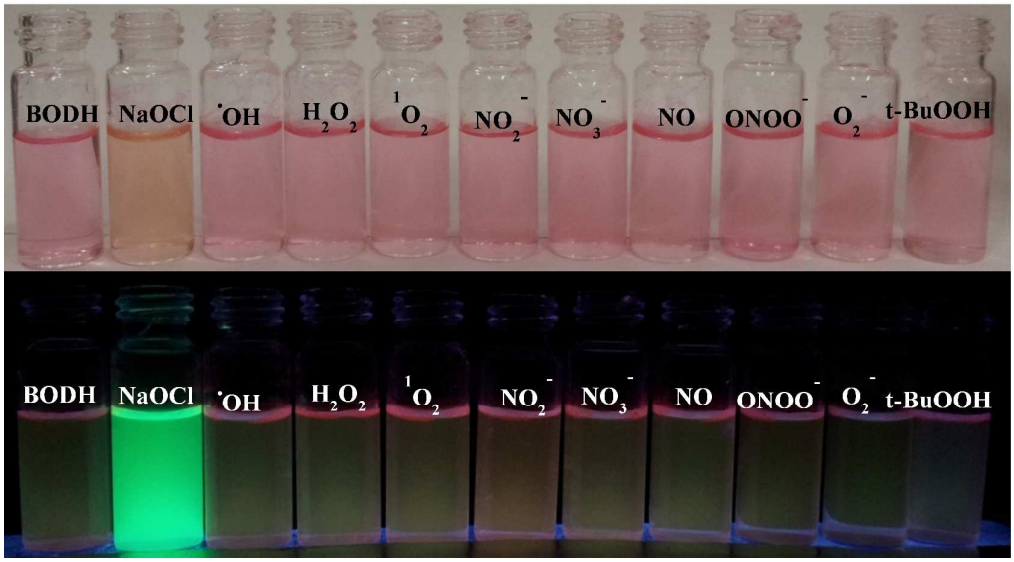

Fig. 1. (a) Color and (b) fluorescence photographs of **BODH** (5 μM) in a PBS buffer-MeOH (v/v = 70/30, 70 mM PBS, pH7.4) solution. **BODH** was excited by UV irradiation (λ_{ex}: 365 nm).

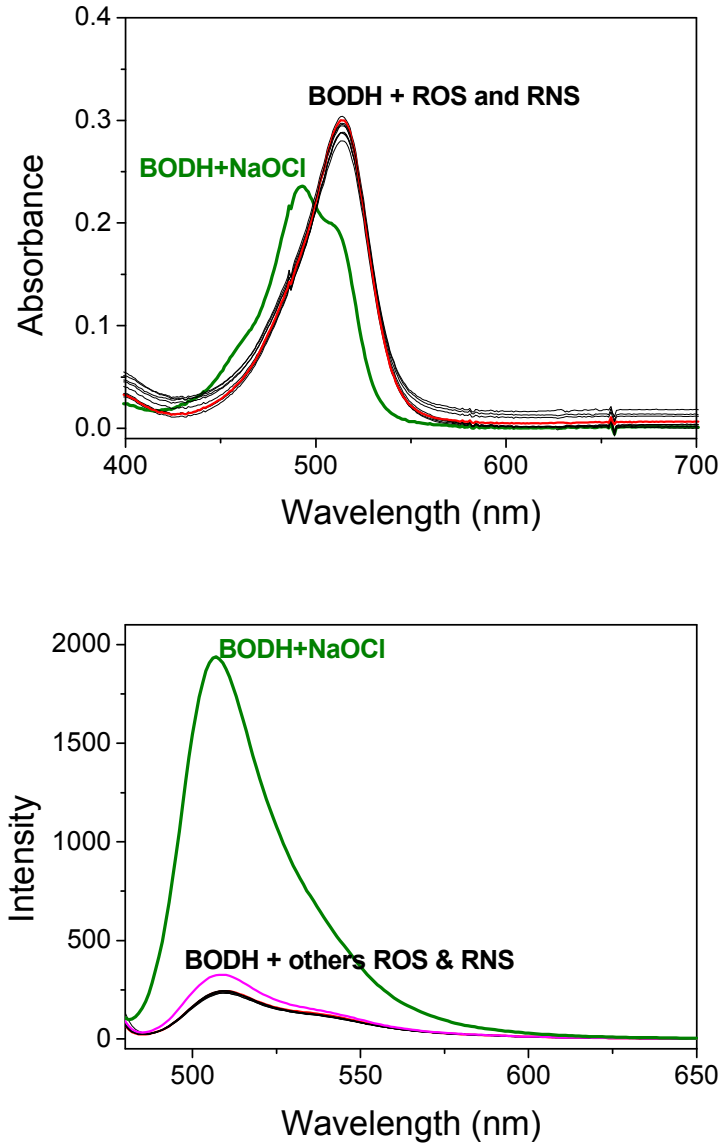

Fig. 2. (a) Absorption spectrum (b) Fluorescence spectra of **BODH** (5 μM) upon adding various ROS & RNS (25 μM) in a H_2O-MeOH (v/v = 70/30, 70 mM PBS, pH7.4) solution. The excitation wavelength was 470 nm.

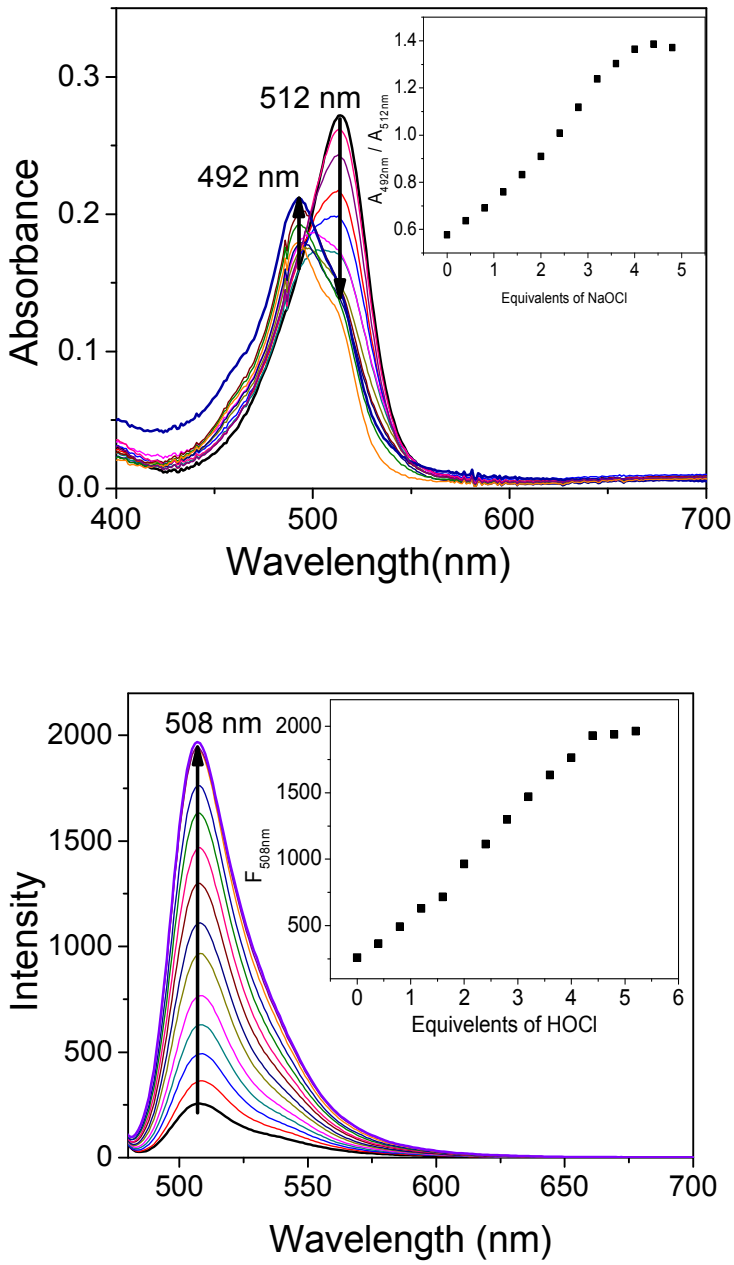

Fig. 3. UV-vis (top) and fluorescence (bottom) changes of **BODH** (5 μM) in the presence of various equivalents of NaOCl in a H_2O-MeOH (v/v = 70/30, 70 mM PBS, pH7.4) solution. The excitation wavelength was 470 nm.

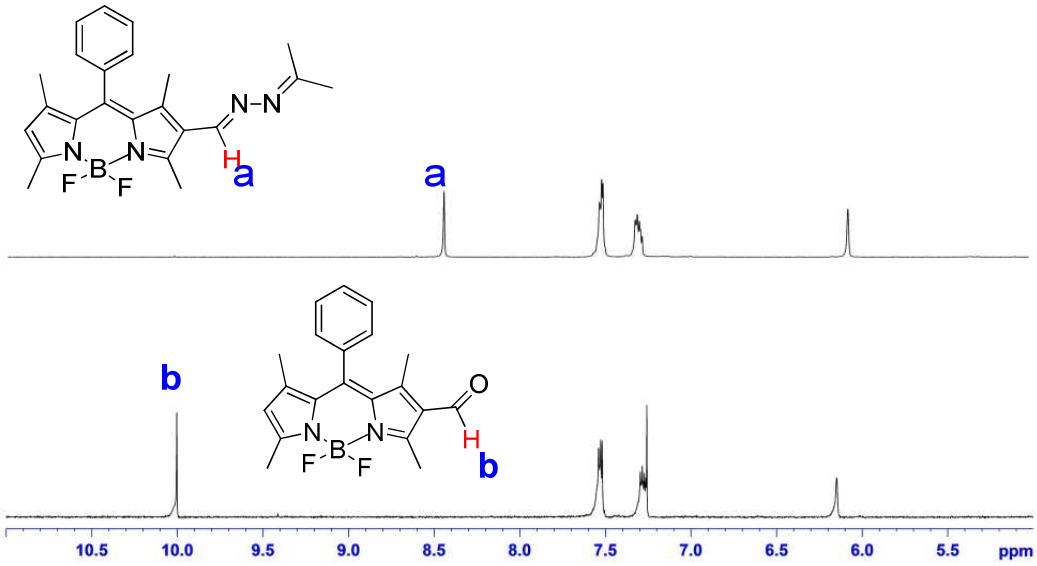

Fig. 4 ^{1}H NMR (500 MHz) spectra of **BDP+HOCl** in $CDCl_3$.

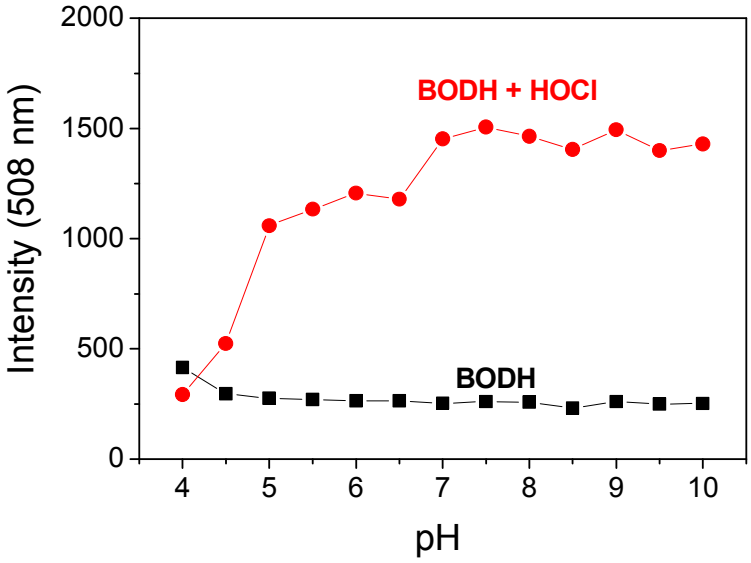

Fig. 5. Fluorescence response (508 nm) of free **BODH** (5 mM) (■) and after addition of NaOCl (25 mM, 5eq) (●) in a H_2O-MeOH (v/v = 70/30, 70 mM buffer) solution as a function of different pH values. The excitation wavelength was 470 nm.

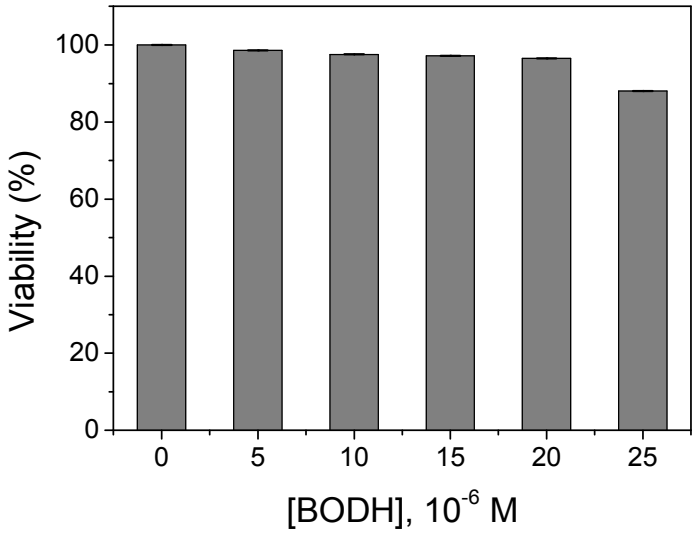

Fig. 6. MTT assay of RAW 264.7 cells were treated in the presence of BODH (0 – 25 μM) incubated for 24 hours.

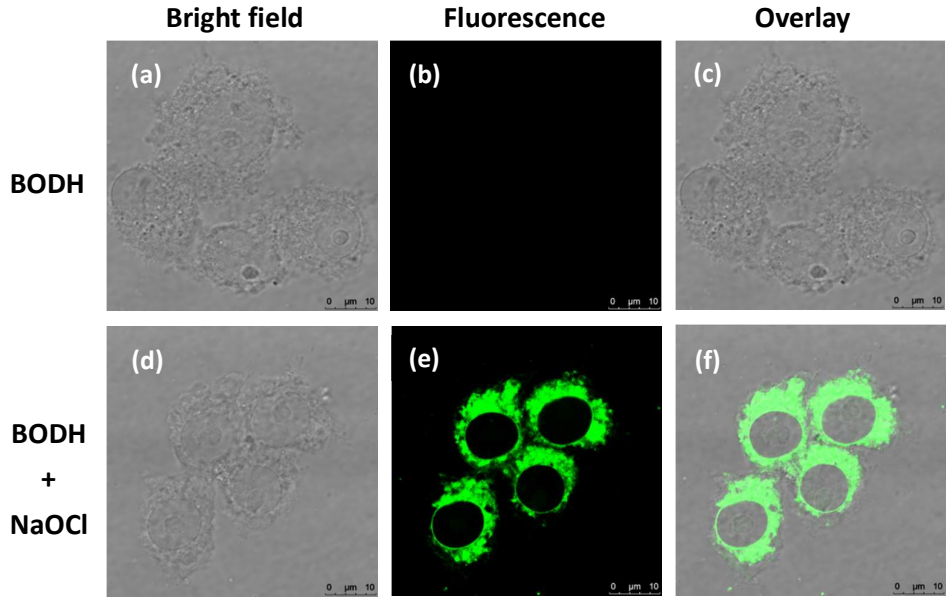

Fig. 7. Confocal fluorescence images of RAW264.7 cells. (a) (d) Bright field image; (b) (e) fluorescence image; and (c) (f)merged image. (a-c) The cells incubated with **BODH** (10 μM) for 30 min. (d-f) Subsequent treatment of the cells with NaOCl (10 μM) for 10 min. Excitation wavelength = 470 nm, scan range = 495-535 nm

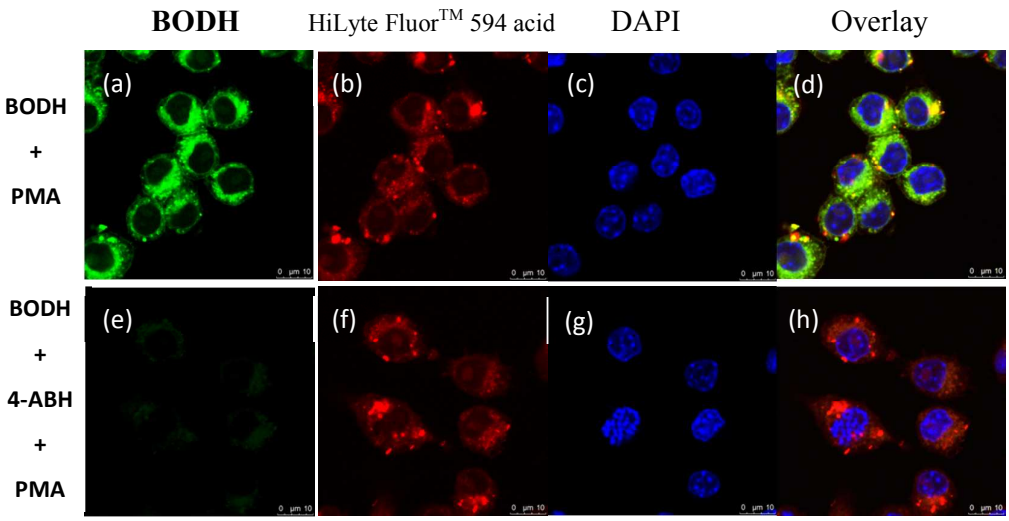

Fig. 8. Detection of PMA-induced hypochlorite production in RAW264.7 cells. (a-d) The cells treated with stimulant PMA (25 ng/mL) for 2 h in the presence of **BODH** (10 μM). (e-f) MPO inhibitor (100 μM), (4-ABH) was co-incubated during PMA stimulation, and incubated with of **BODH** (10 μM) for 1 hour at 37ºC. The cell was colabeled with (b, f) HiLyte Fluor™ 594 acid, (c)(g) DAPI, (e, h) merge image of (a-c) and (e-g). The excitation wavelength for (a, e), (b, f) and (c, g) were 470 nm, 594 nm and 405 nm, respectively; the emission scanning range were 495-535 nm, 637-737 nm and 430-550 nm, respectively.

Figure and Scheme captions

1. **Scheme 1.** Synthesis of the probe **BODH**
2. **Scheme 2.** The reaction of the probe **BODH** with HOCl
3. **Fig. 1.** (a) Color and (b) fluorescence photographs of **BODH** (5 μM) in a PBS buffer-MeOH (v/v = 70/30, 70 mM PBS, pH7.4) solution. **BODH** was excited by UV irradiation (λ_{ex}: 365 nm).
4. **Fig. 2.** (a) Absorption spectrum (b) Fluorescence spectra of **BODH** (5 μM) upon adding various ROS & RNS (25 μM) in a H_2O-MeOH (v/v = 70/30, 70 mM PBS, pH7.4) solution. The excitation wavelength was 470 nm.
5. **Fig. 3.** UV-vis (top) and fluorescence (bottom) changes of **BODH** (5 μM) in the presence of various equivalents of NaOCl in a H_2O-MeOH (v/v = 70/30, 70 mM PBS, pH7.4) solution. The excitation wavelength was 470 nm.
6. **Fig. 4** ^{1}H NMR (500 MHz) spectra of **BDP+HOCl** in $CDCl_3$.
7. **Fig. 5.** Fluorescence response (508 nm) of free **BODH** (5 mM) (■) and after addition of NaOCl (25 mM, 5eq) (●) in a H_2O-MeOH (v/v = 70/30, 70 mM buffer) solution as a function of different pH values. The excitation wavelength was 470 nm.
8. **Fig. 6**. MTT assay of RAW 264.7 cells were treated in the presence of BODH (0 – 25 μM) incubated for 24 hours.
9. **Fig. 7**. Confocal fluorescence images of RAW264.7 cells. (a) (d) Bright field image; (b) (e) fluorescence image; and (c) (f)merged image. (a-c) The cells incubated with **BODH** (10 μM) for 30 min. (d-f) Subsequent treatment of the cells with NaOCl (10 μM) for 10 min. Excitation wavelength = 470 nm, scan range = 495-535 nm
10. **Fig. 8**. Detection of PMA-induced hypochlorite production in RAW264.7 cells. (a-d) The cells treated with stimulant PMA (25 ng/mL) for 2 h in the presence of **BODH** (10 μM). (e-f) MPO inhibitor (100 μM), (4-ABH) was co-incubated during PMA stimulation, and incubated with of **BODH** (10 μM) for 1 hour at 37ºC. The cell was colabeled with (b, f) HiLyte Fluor^{TM} 594 acid, (c)(g) DAPI, (e, h) merge image of (a-c) and (e-g). The excitation wavelength for (a, e), (b, f) and (c, g) were 470 nm, 594 nm and 405 nm, respectively; the emission scanning range were 495-535 nm, 637-737 nm and 430-550 nm, respectively.